

Electronic Supplementary Information for

Characterization of landfill leachate molecular composition using ultrahigh resolution mass spectrometry

Katherine R. Martin^{*a}, Nicole M. Robey^b, Shirley Ma^a, Leanne C. Powers^a, Andrew Heyes^a, Philippe Schmitt-Kopplin^{a,c,d}, William J. Cooper^b, Timothy J. Townsend^b and Michael Gonsior^{*a}

^a University of Maryland Center for Environmental Science, Chesapeake Biological Laboratory, Solomons, Maryland 20688, USA

^b University of Florida, Department of Environmental Engineering Sciences, Gainesville, Florida 32611, USA

^c Helmholtz Zentrum München, Research Unit Analytical BioGeoChemistry, Neuherberg 85764, Germany

^d Technische Universität München, Chair of Analytical Food Chemistry, Freising-Weihenstephan 85354, Germany

*Corresponding authors: Katherine R. Martin (kmartin@umces.edu) and Michael Gonsior (gonsior@umces.edu)

Abbreviations

CAV	cell accelerator voltage
CE	collision energy
CEC	contaminant of emerging concern
CID	collision-induced dissociation
DBE	double bond equivalent
DOC	dissolved organic carbon
EA	elemental analyzer/analysis
EMV	electron multiplier voltage
ESI	electrospray ionization
FT-ICR-MS	Fourier-transform ion cyclotron resonance mass spectrometry
FV	fragmentor voltage
ICP	inductively coupled plasma
IRMS	isotope ratio mass spectrometer/spectrometry
ISTD	internal standard
HPLC	high-performance liquid chromatograph/chromatography
LOD	Limit of detection
MRM	multiple reaction monitoring
MS	mass spectrometer/spectrometry
MS/MS	tandem mass spectrometry
NSAID	nonsteroidal anti-inflammatory drug
QSU	quinine sulfate units
QqQ	triple quadrupole
RT	retention time
SIL	stable isotope-labelled
SPE	solid-phase extract/extraction
TDN	total dissolved nitrogen

Contents

Filtering and SPEs.....	S4
Table S1. Volumes for SPEs	S4
HPLC-MS/MS Methods for Quantification of CECs.....	S4
Table S2. Sources and purities of CEC standards and SIL-ISTDs	S5
Table S3. Separation gradient used in Acesulfame Potassium Method.....	S5
Table S4. Autosampler and LC settings for Acesulfame Potassium Method	S6
Table S5. MS settings for Acesulfame Potassium Method.....	S6
Table S6. MRM settings in Acesulfame Potassium Method.....	S6
Table S7. Separation gradient used in the Other CECs Method.....	S6
Table S8. Autosampler and LC settings for the Other CECs Method	S7
Table S9. MS settings for Other CECs Method.....	S7
Table S10. MRM settings in Other CECs Method	S8
Recovery Experiments for CECs.....	S8
Table S11. Loaded sample volumes for CEC recovery experiments	S9
Table S12. Measured CEC recoveries	S9
Detection Limits for CECs	S10
Table S13. Approximate detection limits	S10
ICP-MS Method	S10
EA-IRMS Method.....	S10
Excitation-Emission Matrices.....	S10
Figure S1. Fluorescence EEMs	S11
Figure S2. LLOM absorbance	S11
Table S14. Optical parameters.....	S12
Quantification of DOC, TDN, Cl ⁻ , NO ₃ ⁻ -NO ₂ ⁻ , and NH ₄ ⁺ /NH ₃	S12
Multiple Formula Assignments for FT-ICR-MS Data	S12
Formula Protocols	S12
<i>m/z</i> Decimal vs. <i>m/z</i> Plots	S13

Figure S3. FT-ICR-MS m/z decimal vs. m/z plots	S13
185.0278 and 417.2283 m/z Ion Peaks	S14
Figure S4. Full FT-ICR-MS spectra	S14
58.0419 m/z and 22.0131 m/z Spacing Patterns	S14
Table S15. Signal intensity for 58.0419 m/z spacing pattern	S14
Table S16. Signal intensity for 22.0131 m/z spacing pattern	S15
Formula Distributions	S16
Table S17. Numbers of formulas in all formula class categories	S16
Table S18. Numbers of unique formulas	S16
Other Halogenated Formula Classes	S16
Figure S5. Van Krevelens of other halogenated formulas	S16
Additional Van Krevelen Diagrams	S17
Figure S6. Van Krevelens of CHOCI for LLOM and SRNOM	S17
Figure S7. Van Krevelens of CHON by nitrogen number	S18
Figure S8. Van Krevelens of CHONS by nitrogen number	S19
$C_9H_4Cl_6O_4$ and Similar Formula Organohalogens	S19
Table S19. Signal intensity data showing isotopic patterns	S19
Table S20. Signal intensity data for the most abundant isotopic peak	S21
Likely Brominated Ions Not Included in Final Dataset	S21
Table S21. Signal intensity data for likely brominated formulas	S21
MS settings for QqQ HPLC-MS-MS Experiments	S21
Table S22. MS settings for QqQ HPLC-MS-MS Experiments	S21
Targeted QqQ HPLC-MS-MS Experiments	S22
Figure S9. Chromatograms for $C_9H_4Cl_6O_4$ in <i>Active</i> LL	S22
Figure S10. Chromatograms for $C_9H_5Cl_5O_4$ in <i>Active</i> LL	S23
Figure S11. Chromatograms for $C_9H_6Cl_4O_4$ in <i>Closed</i> LL	S24
Full Scan Mode QqQ HPLC-MS-MS Experiments	S25
Figure S12. Spectrum for $C_9H_4Cl_6O_4$, in <i>Active</i> LL	S25
Figure S13. Spectrum for $C_9H_5Cl_5O_4$, in <i>Active</i> LL	S25
Figure S14. Spectrum for $C_9H_5Cl_5O_4$ in <i>Closed</i> LL	S26
Figure S15. Spectrum for $C_9H_6Cl_4O_4$ in <i>Closed</i> LL	S26
Orbitrap MS-MS Experiments	S27
Table S23. Spectra ion lists for $C_9H_5Cl_5O_4$ in <i>Active</i> LL	S27
Table S24. Spectra ion lists for chlorendic acid standard ($C_9H_4Cl_6O_4$)	S28
References	S29

Filtering and SPEs

Whole leachate was filtered by vacuum filtration using base-washed filter holders. HCl for sample acidification was a pure grade, 32% solution. A mixed-mode reversed-phase, weak anion exchange extraction was used for acesulfame potassium because acesulfame is an acidic anion and because of previous unpublished recovery estimates which showed poor recovery by Agilent Bond Elut PPL. Methanol and 0.1% (v/v) formic acid water used in SPEs were LC-MS grade. Water was ultrapure water generated from an in-lab system. The NH₄OH MeOH was approximately 92% methanol, 8% water and was made by diluting reagent grade, NH₄OH water solutions with methanol. SPEs were done on a vacuum manifold. For the PPL extractions, the larger volume wash step after sample loading was done by putting the formic acid water wash in a combusted glass vial (500 °C) and sending it by peristaltic pump through acid-washed tubing connected with base-washed tube adaptors to the cartridges. Samples were eluted into either new, trace contaminant certified or acid-washed and combusted amber vials with new or base washed caps. SPEs were stored at -20 °C between analyses.

Table S1. Volume of leachate loaded onto cartridges for triplicate SPEs. Cartridges were not loaded with >18 mg DOC/ 1 g sorbent. Concentration factors of extracts are (loaded volume (mL) / elution volume (mL)).

Extraction	Loaded Sample Volume (mL)		
	1	2	3
PPL			
Active	12	16	11.5
Closed	10	10	10
Closed-Brine	11.5	11.5	12
WAX			
Active	2	2	2
Closed	2	2	2
Closed-Brine	2	2	2

HPLC-MS/MS Methods for Quantification of CECs

The carrier gas was high purity nitrogen from a nitrogen generator and the collision gas was ultra-high purity nitrogen. An ISTD quantification method was used to control for fluctuations in instrument performance. All blanks, calibration standards, quality control standards, and samples were spiked with ISTDs. A separate method was used to account for the different SPE matrix of the WAX extracts. Here, the two HPLC-MS/MS methods are referred to as Acesulfame Potassium Method and Other CECs Method. Qualifier transitions were used to further confirm identities of measured compounds. Significant qualifier transitions using different fragment ions were not found for ibuprofen or triclosan. Ibuprofen was run without a qualifier, while a different isotopic transition was used as a qualifier for triclosan because it has three chlorine atoms.

Table S2. Sources and purities of CEC standards and SIL-ISTDs. Purities are guaranteed from the manufacturer or from lot assays as available. Original compound purity is not available for most SIL-standards.

^a Sigma-Aldrich

^b Toronto Research Chemicals

^c CDN Isotopes

^d Cerilliant

CEC	Standard	Source/Purity	Description	SIL-ISTD	Source/Isotopic Purity
acesulfame potassium	acesulfame potassium	99.9% ^a	artificial sweetener	acesulfame potassium-d4	≥98.0% ^b
acetaminophen	acetaminophen	≥98.0% ^a	NSAID	acetaminophen-d3	99.2% ^c
carbamazepine	carbamazepine	99.7% ^d	prescription drug	carbamazepine-d10	98.0% ^b
cotinine	(-)-cotinine	99.5% ^a	nicotine metabolite	(±)-cotinine-d3	99.8% ^c
ibuprofen	ibuprofen	99.7% ^a	NSAID	ibuprofen-13C,d3	98.6% ^b
methylparaben	methylparaben	98.5% ^a	antimicrobial	ethylparaben-d4	98.7% ^c
propylparaben	n-propylparaben	99.9% ^a	antimicrobial	n-propylparaben-d4	98.8% ^c
paraxanthine	paraxanthine	>99.9% ^d	caffeine metabolite	paraxanthine-d3	99.8% ^b
sucralose	sucralose	99.2% ^a	artificial sweetener	sucralose-d6	95.2% ^b
sulfamethoxazole	sulfamethoxazole	≥98.0% ^a	prescription drug	sulfamethoxazole-d4	98.9% ^c
triclosan	triclosan	99.9% ^a	antimicrobial	triclosan-d3	97.5% ^b

Quantification of Acesulfame Potassium

Table S3. Separation gradient used in Acesulfame Potassium Method, where mobile phase A is LC-MS grade methanol and mobile phase B is 0.1% (w/w) ammonium acetate water made by adding ≥99.0% purity ammonium acetate to ultrapure water. Flow after 4 minutes was sent to waste using the divert valve.

Time (min)	A (%)	B (%)
0.00	90.0	10.0
4.00	90.0	10.0
5.00	60.0	40.0
6.00	60.0	40.0
7.00	90.0	10.0
10.00	90.0	10.0

Table S4. Autosampler and LC settings for Acesulfame Potassium Method.

Parameter	Setting
Flow	0.250 mL/min
Column Temperature	50 °C
Injection Volume	3 uL
Needle Wash	Flush Port = 10 s
Draw Speed	200 uL/min
Eject Speed	400 uL/min
Wash time after draw	1.2 s
Needle height offset	0.0 mm
Sample Flush-out factor	5 times injection volume

Table S5. MS settings for Acesulfame Potassium Method.

Parameter	Setting
Ion source	ESI
Capillary voltage	Positive = 4000 V, Negative = 2500 V
Gas temperature	350 °C
Gas flow	10 L/min
Nebulizer gas pressure	40 psi
MS1/MS2 resolution	Unit
Time filtering	peak width = 0.03 min
Scan type	MRM
Delta EMV (-)	400 V

Table S6. MRM settings in Acesulfame Potassium Method.

Compound	Transition Type	Ion Mode	Transition	RT (min)	FV (V)	CE (V)	CAV (V)
acesulfame potassium	target	negative	162.0 → 82.0	1.50	80	10	7
acesulfame potassium	qualifier	negative	162.0 → 78.0	1.50	80	34	7
acesulfame potassium-d4	ISTD	negative	166.0 → 86.0	1.50	80	10	7

Quantification of Other CECs

Table S7. Separation gradient used in the Other CECs Method, where mobile phase A is LC-MS grade methanol and mobile phase B is 0.1% (v/v) LC-MS grade formic acid water. Flow after 8 minutes was sent to waste using the divert valve.

Time (min)	A (%)	B (%)
0.00	50.0	50.0
0.10	50.0	50.0
0.20	97.0	3.0
7.00	97.0	3.0
8.00	50.0	50.0

Table S8. Autosampler and LC settings for the Other CECs Method.

Parameter	Setting
Flow	0.3 mL/min
Column Temperature	50 °C
Injection Volume	5 uL
Needle Wash	Flush Port = 10 s
Draw Speed	200 uL/min
Eject Speed	400 uL/min
Wash time after draw	1.2 s
Needle height offset	0.0 mm
Sample Flush-out factor	5 times injection volume

Table S9. MS settings for Other CECs Method.

Parameter	Setting
Ion source	ESI
Capillary voltage	Positive = 5000 V, Negative = 2600 V
Gas temperature	350 °C
Gas flow	10 L/min
Nebulizer gas pressure	35 psi
MS1/MS2 resolution	Unit
Time filtering	peak width = 0.03 min
Scan type	dynamic MRM
Delta EMV (+/-)	400 V

Table S10. MRM settings in Other CECs Method.

Compound	Transition Type	Ion Mode	Transition	RT (min)	FV (V)	CE (V)	CAV (V)
acetaminophen	target	Positive	152.0 → 110.2	1.90	110	16	2
acetaminophen	qualifier	Positive	152.0 → 65.0	1.90	110	35	2
acetaminophen-d3	ISTD	positive	155.2 → 111.0	1.88	110	16	2
carbamazepine	target	positive	237.0 → 194.0	4.73	160	18	4
carbamazepine	qualifier	Positive	237.0 → 179.0	4.73	160	18	4
carbamazepine-d10	ISTD	Positive	247.2 → 204.2	4.7	160	18	4
cotinine	target	Positive	177.2 → 80.2	1.74	90	22	3
cotinine	qualifier	Positive	177.2 → 98.1	1.74	90	22	3
cotinine-d3	ISTD	Positive	180.2 → 101.0	1.74	90	22	3
ibuprofen	target	Positive	207.2 → 161.1	5.56	100	3	3
ibuprofen	qualifier	NA	NA	NA	NA	NA	NA
ibuprofen-13C,d3	ISTD	positive	211.3 → 165.3	5.58	100	7	3
methylparaben	target	positive	153.0 → 121.0	4.40	110	18	3
methylparaben	qualifier	positive	153.0 → 65.0	4.40	110	30	3
ethylparaben-d4	ISTD	positive	171.0 → 99.2	4.8	80	18	3
propylparaben	target	positive	181.0 → 95.0	5.12	80	18	3
propylparaben	qualifier	positive	181.0 → 121.0	5.12	80	18	3
propylparaben-d4	ISTD	positive	185.0 → 99.2	5.11	80	18	3
paraxanthine	target	positive	181.1 → 124.1	2.00	90	23	3
paraxanthine	qualifier	positive	181.1 → 96	2.00	90	23	3
paraxanthine-d3	ISTD	Positive	184.1 → 127.1	1.99	90	23	3
sucralose	target	positive	419.0 → 221.0	2.36	160	15	7
sucralose	qualifier	Positive	419.0 → 239.0	2.36	160	15	7
sucralose-d6	ISTD	Positive	425.0 → 223.0	2.34	160	15	7
sulfamethoxazole	target	Positive	254.0 → 92.0	2.69	110	25	4
sulfamethoxazole	qualifier	Positive	254.0 → 156.0	2.69	110	15	4
sulfamethoxazole-d4	ISTD	Positive	258.1 → 160.1	2.67	110	15	4
triclosan	target	negative	289.0 → 37.0	6.35	80	8	4
triclosan	qualifier	negative	287.0 → 35.0	6.35	80	8	4
triclosan-d3 1	ISTD	negative	292.0 → 37.0	6.34	80	8	4

Recovery Experiments for CECs

Recovery experiments were conducted after initial quantification of CECs by spiking *Active* and *Closed* whole leachate samples with analytical standards and measuring spike recovery by triplicate SPEs comparable to original extraction procedures. Whole leachates were re-extracted in triplicate as a base level to account for any degradation/sorption between original extractions (PPL: 05/2018; WAX: 06/2019) and recovery experiments (11/2019-12/2019). Whole leachates were filtered again, spiked as applicable, and acidified as described in the article methods. WAX spikes (acesulfame potassium) were approximately 1500 µg/L for the *Active* sample and 50 µg/L for the *Closed* sample. PPL spikes (other CECs) were chosen to be approximately 100 µg/L for non-detect measurements or measurements at <50 µg/L, or 1000 µg/L for all other measurements. All spikes were within calibration curves at the same dilution levels as the original quantification. The same cartridge types were used for the equivalent recovery experiments and all extraction steps remained the same.

Table S11. Loaded sample volumes for CEC recovery experiments. All PPL cartridges were eluted with 10 mL MeOH. All WAX cartridges were eluted with 3 mL of the NH₄OH MeOH solution.

Extraction	Loaded Sample Volume (mL)		
	1	2	3
PPL			
Active	10	10	10
Closed	10	10	10
Active-spike	10	10	10
Closed-spike	10	10	10
WAX			
Active	2	2	2
Closed	3	3	3
Active-spike	2	2	2
Closed-spike	3	3	3

Table S12. Measured CEC recoveries calculated as % of spike addition detected over base level.

CEC	SPE Recovery (%)					
	Active			Closed		
	1	2	3	1	2	3
PPL						
acetaminophen	104	119	120	118	130	121
carbamazepine	102	113	113	115	127	117
cotinine	102	114	111	108	126	112
ibuprofen	99	113	112	107	118	108
methylparaben	91	127	104	111	141	122
propylparaben	92	110	108	121	141	117
paraxanthine	101	116	112	110	122	115
sucralose	109	122	107	159	150	139
sulfamethoxazole	67	76	74	25	30	26
triclosan	42	50	38	44	46	45
WAX						
acesulfame potassium	76	91	84	80	105	78

Detection Limits for CECs

Table S13. Approximate LOD is the lowest standard included in the quantification standard curve. Approximate matrix detection limits were calculated as [concentration of lowest standard curve level ($\mu\text{g/L}$) \times maximum LLOM dilution factor] \div [minimum measured recovery (%)/100]. Measured recoveries $>100\%$ were considered as 100%.

CEC	~Limit of Detection ($\mu\text{g/L}$)	~Matrix Detection Limit ($\mu\text{g/L}$)
acesulfame potassium	0.125	5.7
acetaminophen	0.25	8.7
carbamazepine	0.05	1.7
cotinine	0.05	1.7
ibuprofen	0.075	2.6
methylparaben	2	76.4
propylparaben	0.45	17.0
paraxanthine	0.55	19.1
sucralose	3	104.3
sulfamethoxazole	0.06	8.3
triclosan	0.125	11.4

ICP-MS Method

The acidification of samples resulted in precipitation of organic matter that would interfere with analysis. As a result, the samples required stronger digestion before analysis. This was done using a Milestone EOTHO-EZ microwave. 20 mL quartz reaction vessels were placed inside Teflon cups, which pressure seal during digestion. For this digestion the 2 mL of sample was placed in the quartz vessel with 2 mL of concentrated ultrapure nitric acid and 6 mL of ultrapure water. 5 mL of 30% hydrogen peroxide was added to the Teflon cup along with 5 mL of ultrapure water, and the cup was sealed. The samples were heated to 180 °C and allowed to reflux for 15 minutes then diluted to 10 mL with ultrapure water. These were diluted and analyzed for trace elements. For analysis of the SPEs, 1 mL of extract was placed in a glass vial and evaporated to dryness. 2 mL of nitric acid was added to the vial and swirled, capped, and left for 24 hrs. 8 mL of ultrapure water was added to the vial, and the sample was further diluted prior to analysis.

The standards used for ICP-MS analysis were made from Multi-Element Solution 2A (Spex CertiPrep) and the internal standard used was ICP-MS Alternate Internal Standard 1 (Spex CertiPrep), containing ^6Li , Sc, Ge, Y, In, Tb, and Bi. The ICP-MS used was an Agilent 7500C. All elements except Cd and Pb were measured using helium in the collision cell in order to reduce interferences. Detection limits for each element are listed in parentheses: Mn (0.1), Fe (0.5), Cd (0.01), Pb (0.01), V (0.04), Cr (0.03), Cu (0.02), Zn (3.9), As (0.04) in $\mu\text{g/L}$. All samples were spiked with standard to test recoveries by standard addition. Recoveries ranged from 92 to 100%.

EA-IRMS Method

Standards were acetanilide and bass protein lab standards calibrated against USGS40 and USGS41a (Reston Stable Isotope Laboratory). Molar C/N is from the higher volume, $\delta^{15}\text{N}$ analysis.

Excitation-Emission Matrices

Dilution factors of 1:420, 1:110, and 1:130 were used for the *Active*, *Closed*, and *Closed-Brine* LL samples respectively. Raman, first-order Rayleigh, and second-order Rayleigh scatter was corrected and EEMs were smoothed. Values have been corrected for dilution and fluorescence was converted to QSU using a 1 mg/L quinine sulfate reference standard (Starna).

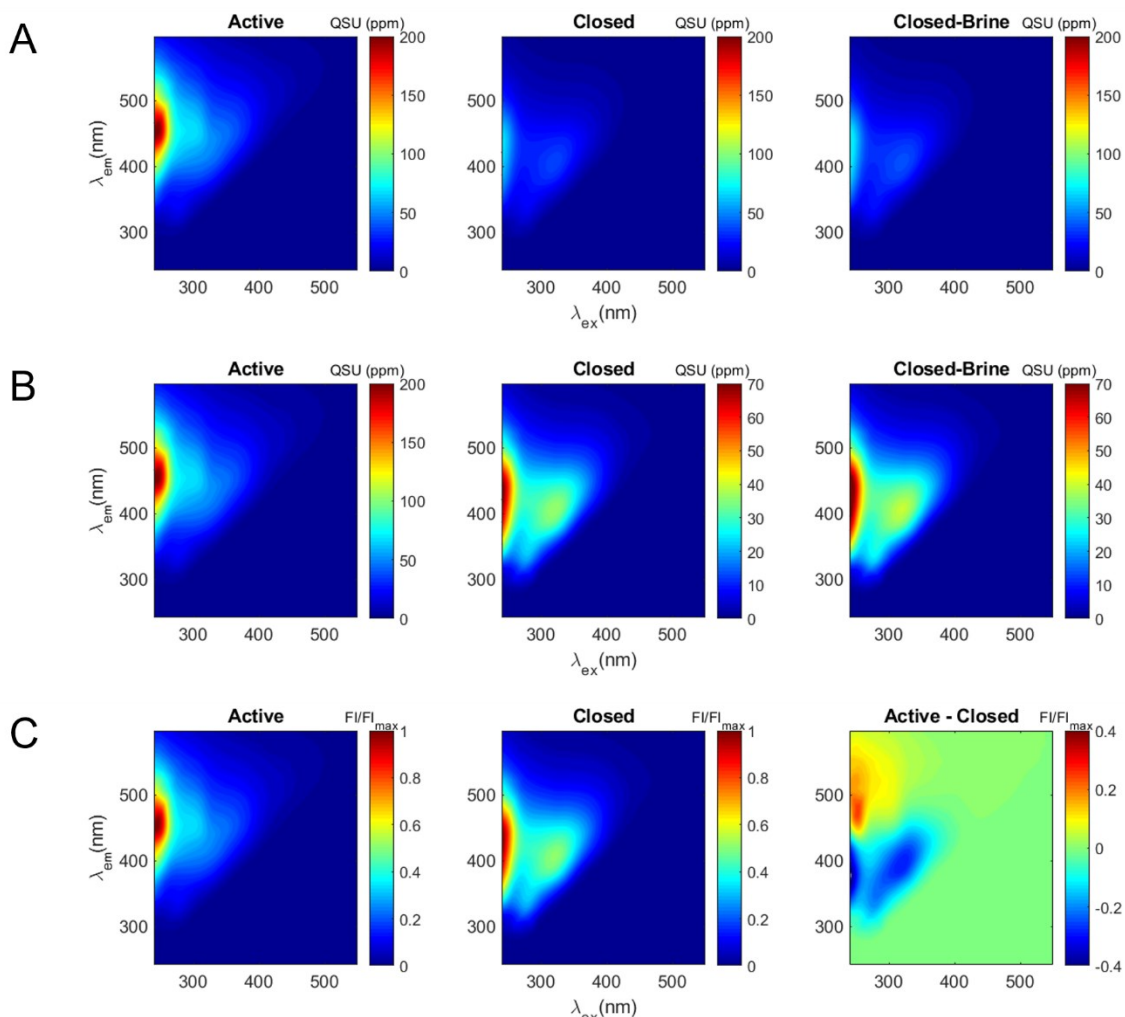


Figure S1. Fluorescence EEMs of *Active*, *Closed*, and *Closed-Brine* LL samples on the same fluorescence scale (A). Fluorescence EEMs of *Active*, *Closed*, and *Closed-Brine* LL samples on separate fluorescence scales (B). Fluorescence normalized to max fluorescence for the *Active* and *Closed* LL samples and normalized *Active* LL subtracting normalized *Closed* LL (C).

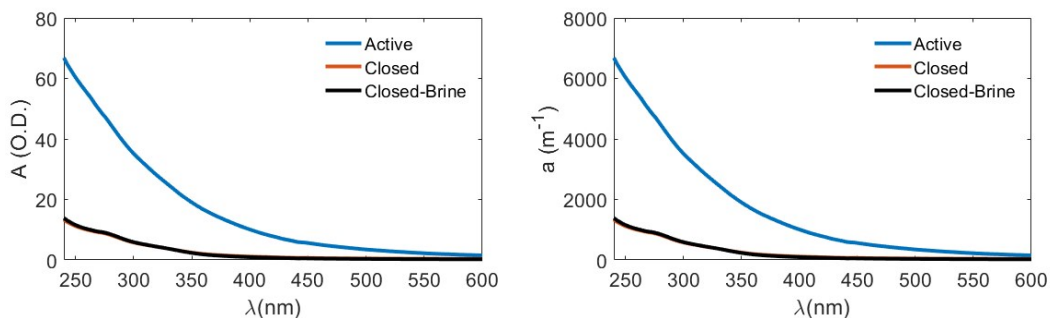


Figure S2. Raw absorbance as optical density (left) and absorbance as decadic absorption coefficient (right).

Table S14. Optical parameters where S is spectral slope¹ between the stated wavelengths, S_R is spectral slope ratio as (S₂₇₅₋₂₉₅/S₃₅₀₋₄₀₀), A₂₅₄ is raw absorbance at 254 nm, Dec. a₂₅₄ is decadic absorption coefficient at 254 nm, and SUVA₂₅₄ is the specific UV absorbance at 254 nm.²

Parameter	Active	Closed	Closed-Brine
S ₃₀₀₋₆₀₀ (nm ⁻¹)	0.011	0.009	0.011
S ₂₇₅₋₂₉₅ (nm ⁻¹)	0.012	0.017	0.017
S ₃₅₀₋₄₀₀ (nm ⁻¹)	0.013	0.015	0.018
S _R	0.971	1.138	0.978
A ₂₅₄ (O.D.)	58.219	10.639	10.953
Dec. a ₂₅₄ (m ⁻¹)	5821.918	1063.878	1095.266
SUVA ₂₅₄ (L mg ⁻¹ m ⁻¹)	5.577	1.976	1.671

Quantification of DOC, TDN, Cl⁻, NO₃⁻-NO₂⁻, and NH₄⁺/NH₃

All LL samples were diluted at a 1:40 dilution factor before analyses and reported values were corrected for this. Carbon standard for DOC was potassium hydrogen phthalate (Sigma-Aldrich, ≥99.5% purity). Nitrogen standard for TDN was potassium nitrate (Acros Organics, ≥99% purity). Blanks, standards, and samples were all acidified to pH 2 with pure grade HCl before DOC and TDN analyses. Other analytes run by Nutrient Analytical Services Laboratory, Chesapeake Biological Laboratory (MD, USA). For NO₃⁻-NO₂⁻ the given method reporting limit/method detection limit was 0.028/0.0057 mg N/L or approximately 1.12/0.228 mg N/L when considering the 1:40 dilution factors.

Multiple Formula Assignments for FT-ICR-MS Data

NetCalc uses a network assignment approach that does not allow for multiple formula assignments for the same *m/z* ion, but because network assignments were done individually by sample there was some possibility of multiply assigned ions. Thirty-four ions were doubly assigned across samples, twenty-one of which fell under the final 600 *m/z* cutoff. No ions were triply assigned. For most of these the clear, more likely, formula assignments based on mass error, isotopic patterns, and fewer heteroatoms were chosen, but a common mass overlap was found between the CHON₂Cl₁ and CHOS₁ formulas. This is caused by the similarity of H₃O₄S (98.9757529) vs C₃N₂Cl (98.9755493). For this reason, the final dataset has N₁Cl₁ and N₃Cl₁ formula assignments in the CHONCl class, but N₂Cl₁ assignments were removed. Evidence against the N₂Cl₁ assignments was that higher signal intensity ions assigned as this type did not have ³⁷Cl isotopic peaks when expected with no obvious overlap to obscure the isotopic peaks. This evidence favors the CHOS assignments in cases of multiple formula assignments. Logically, some CHON₂Cl₁ formulas must be present for the existence of CHON₃Cl₁, but the lower intensity N₂Cl₁ assignments that did not belong to multiply assigned ions, though plausible, were removed because they could not be verified from their corresponding possible CHOS assignments. This overlap did not seem to continue to the N₃Cl₁ assignments, where a mass overlap of CHON₁S₁ with CHON₃Cl₁ might be expected. The high intensity N₃Cl₁ peaks had corresponding ³⁷Cl isotopic peaks at expected ratios.

Formula Protocols

Final formula assignments have only positive, integer DBEs and do not violate the nitrogen rule. All 2- and 4-N assignments correspond to even integer neutral masses, and all 1- and 3-N assignments correspond to odd integer neutral masses. All assignments containing only C, H, O, S, P, or halogens correspond to even integer neutral masses. Final formula assignments all have O/C ≤ 1 and ≥ 0.05, H/C > 0.3, N/C ≤ 1, H ≤ (2C + 2 + N), and O ≤ (C + 2), following commonly used filtering protocols.^{3,4} Final formula assignment N/C is between 0-0.3.

m/z Decimal vs. *m/z* Plots

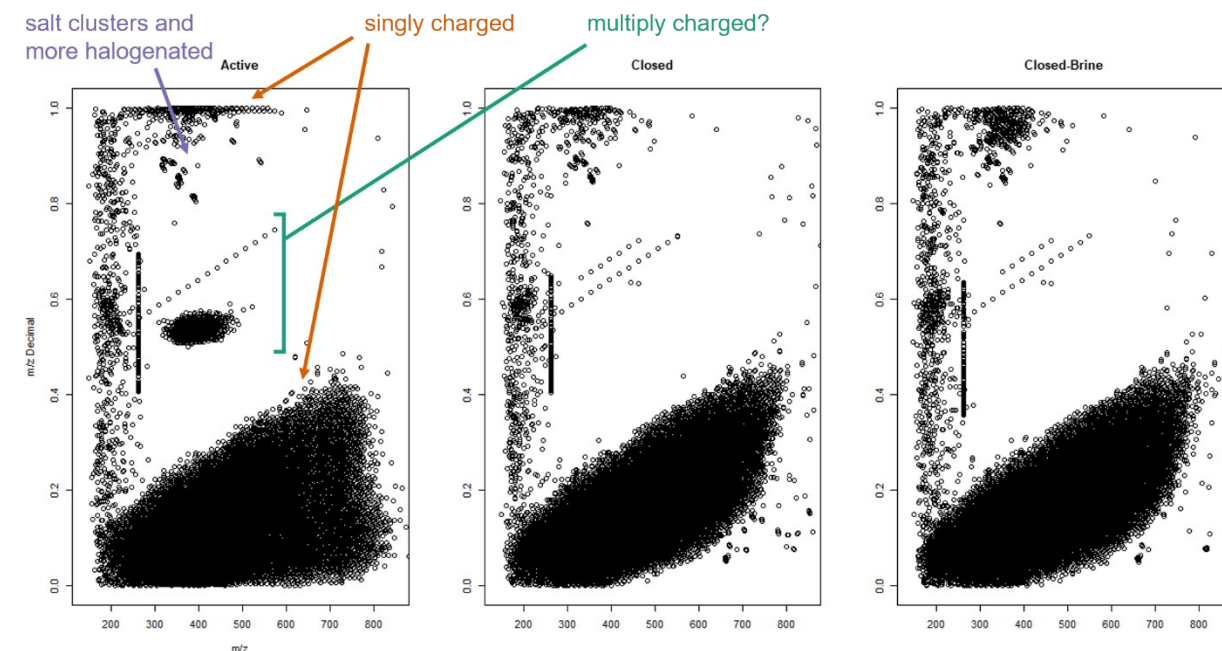


Figure S3. *Active*, *Closed*, and *Closed-Brine* *m/z* decimal vs. *m/z* plots, following McMillan et al.,⁵ made using unassigned, signal intensity averaged data matrix, including ions not measured in all triplicates. The multiply charged cluster distinct to the *Active* LL sample appears to be doubly charged ions corresponding to the one ¹³C isotopic peak of a group of >600 *m/z*, singly charged, CHO ions. Doubly charged ions of the singly charged, monoisotopic peaks are also present but have mass decimals within the singly charged window, so are not distinguishable in the figure. The singly charged formulas believed to correspond are approximately 0.75 H/C, 0.5 O/C, and have low *m/z* decimals. This group, and the high mass, low *m/z* decimal region of ions in the *Active* LL sample in general, should be a subject of further study. The linear homologous series in the “multiply charged” decimal region, one in the *Active* LL and two in the *Closed* and *Closed-Brine* LL samples, have 22.0131 *m/z* spacing patterns, and we believe these are doubly charged ethylene oxide (44.0262 *m/z*, CH₂CH₂O) series. The small *m/z* spaced linear series in the “singly charged”/“salt clusters and more halogenated” region are 1.9970 *m/z*, Cl and 1.9980 *m/z*, Br isotopic patterns and are highly substituted organohalogenes. Highly fluorinated, singly charged ions also plot in this region. The vertical, linear feature at approximately 262.5 *m/z* is a known instrument artifact.

185.0278 and 417.2283 m/z Ion Peaks

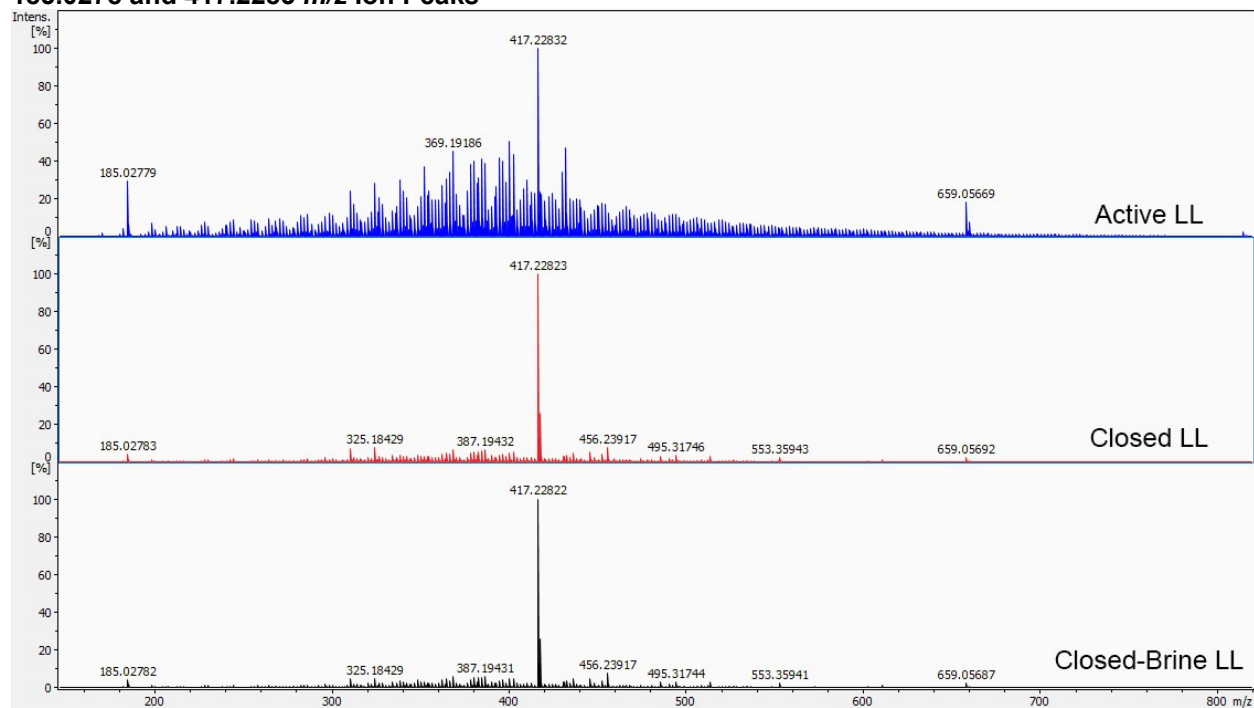


Figure S4. Full spectra of representative LL samples showing 185.0278 and 417.2283 m/z ion peaks. Relative intensity is as % of the base peak.

58.0419 m/z and 22.0131 m/z Spacing Patterns

Table S15. Signal intensity data in arbitrary units from the unprocessed data matrix showing the 58.0419 m/z spacing pattern seen in LLOM Van Krevelen diagrams at $H/C = 2$. We believe this spacing represents propylene oxide $[CH_2CH(CH_3)O]$ units. Formula assignments and mass error are given, but not every ion in the series was included in the final dataset due to mass cutoffs. Molecular characterization is non-structural, but the formulas in the series, interestingly, are the same as known monocarboxylated polypropylene glycols that Rogers et al.⁶ identified as polypropylene glycol degradation products. Further analyses are needed for any actual structural identification, but future studies could explore this.

m/z (avg.)	Neutral Mass (Da)	Closed 3	Closed 2	Closed 1	Closed-Brine 3	Closed-Brine 2	Closed-Brine 1	Active 3	Active 2	Active 1	Formula	Error (ppm)
205.10814	206.11541	67852216	65962500	68244320	69225376	68378296	67495024	23479682	23104544	25695702	$C_9H_{18}O_5$	0.07
263.15001	264.15729	78334232	75619512	93037392	95281320	88424872	92152440	49800188	46577104	58985840	$C_{12}H_{24}O_6$	0.01
321.19189	322.19916	217510032	211008576	231359136	233065872	223496000	232897472	106577056	99940696	111281664	$C_{15}H_{30}O_7$	0.03
379.23367	380.24095	420118784	396005152	448960256	445561536	420853760	451843168	161805904	148984256	178470960	$C_{18}H_{36}O_8$	0.19
437.27568	438.28296	418919328	396441472	456347008	458718336	444891424	467750496	132004032	116536720	147835056	$C_{21}H_{42}O_9$	0.16
495.31744	496.32472	310886080	297842592	328262144	323221728	319677920	334547712	88002848	72415800	97085112	$C_{24}H_{48}O_{10}$	0.06
553.35942	554.36669	212087952	202552688	240801792	236346240	229916672	236014592	46482152	43017660	50360172	$C_{27}H_{54}O_{11}$	0.14
611.40138	612.40866	116858752	111321088	130495520	127251968	123022832	130500272	22242016	18790498	25594906	$C_{30}H_{60}O_{12}$	0.29
669.44314	670.45041	51338496	46461144	54713220	52598912	53124616	58302560	8270220	7349626	9907421	$C_{33}H_{66}O_{13}$	0.10
727.48504	728.49231	17387626	14427860	17451072	16323350	16705752	17150874	3967939	3404953	5245720	$C_{36}H_{72}O_{14}$	0.14
785.52718	786.53445	3048311	3257178	4668662	3727650	3785597	4303722	0	0	0	$C_{39}H_{78}O_{15}$	0.48

Table S16. Signal intensity data in arbitrary units from the unprocessed data matrix showing the 22.0131 m/z spacing pattern seen in m/z decimal vs. m/z plots. We believe these are doubly charged ions and the corresponding singly charged m/z spacing would be 44.0262 m/z , likely ethylene oxide ($\text{CH}_2\text{CH}_2\text{O}$) units. We believe “Series 1” could be doubly charged CHON ions, where the 242.548 m/z ion would be doubly deprotonated $\text{C}_{23}\text{H}_{21}\text{NO}_{11}$, with the other series formulas following the $+\text{C}_2\text{H}_4\text{O}$ pattern. “Series 2” could be doubly charged, one ^{13}C ions, where the 330.644 m/z ion would be doubly deprotonated $^{12}\text{C}_{26}^{13}\text{CH}_{50}\text{O}_{18}$, with the other series formulas following the $+^{12}\text{C}_2\text{H}_4\text{O}$ pattern. These assignments have reasonable mass error, as the average mass error is 0.5 ppm for the “Series 1” assignments and 0.1 ppm for the “Series 2” assignments. This is our current best, but preliminary, understanding based on corresponding singly charged formula assignments and m/z ions for “Series 1” and corresponding singly charged m/z ions; doubly charged, monoisotopic m/z ions; and singly charged, monoisotopic m/z ions for “Series 2”.

m/z (avg.)	Closed 3	Closed 2	Closed 1	Closed-Brine 3	Closed-Brine 2	Closed-Brine 1	Active 3	Active 2	Active 1
Series 1									
242.54816	0	0	0	0	0	2137647	0	1694626	0
264.56135	0	0	0	0	0	2110252	0	2033392	0
286.57448	2358242	2650029	0	2663982	2908474	2534715	2956017	2806082	2625640
308.58757	4507414	5163214	4841418	4062526	5317520	4873693	4672188	4565506	5560497
330.60064	7209036	7536954	7852868	8073698	8189627	9290743	7651678	8288083	7827040
352.61374	10068126	9614192	9587009	11400531	10775060	11161236	10922593	12142078	11343610
374.62690	12667240	10007515	10942243	11731192	11023662	11531185	13134411	16126356	13704150
396.64000	14766681	12881492	12955909	13931315	13184135	14342559	17770594	19670432	17849336
418.65312	14046840	11419255	12768891	14112148	11387536	13590834	14567060	16772714	16280733
440.66623	13028552	11515873	13829915	15740329	14258615	14393151	16895696	20370492	17567490
462.67933	9698504	10117837	9706141	11164203	10637038	12126784	14497692	16537918	15346020
484.69242	9113498	6687133	9171263	9268702	8757239	9950836	11911092	13250079	12991395
506.70562	7574209	5871404	6445912	7678060	7550081	6824286	10408285	11422973	10398072
528.71871	5395387	4756049	5284161	6012281	6783027	5951607	8298198	9072633	8691347
550.73188	0	0	3919683	3900163	4446978	3886463	6333157	7289357	5852649
572.74491	0	0	0	0	0	0	4271517	4767705	4157758
Series 2									
330.64426	0	2626405	0	0	0	0	0	0	0
352.65736	5009094	4861336	4851562	3398529	3892802	4753086	0	0	0
374.67043	8469902	7820289	6251338	6892836	4739420	5609434	0	0	0
396.68361	8068733	8753782	8491305	6395739	6042802	6216133	0	0	0
418.69675	7052953	7635606	7637662	5971383	4476084	6839636	0	0	0
440.70982	6272230	6885373	7344954	5172679	4746706	6132572	0	0	0
462.72297	4393187	4553446	4341946	0	0	3995736	0	0	0

Formula Distributions

Table S17. Numbers of formulas in formula classes in molecular characterization of LL and comparison to SRNOM. A conservative approach was used for SRNOM formula assignment filtering for comparison purposes.

	Active LL	Closed LL	Closed-Brine LL	SRNOM
CHO	2547	2362	2392	2925
CHON	2688	3307	3295	1439
CHOS	1161	1213	1253	255
CHONS	592	1072	1072	14
CHOCI	674	830	863	136
CHONCI	90	206	215	7
CHOSCI	10	30	33	14
CHONSCI	1	12	13	0
CHOF	3	3	3	0
CHOSF	2	3	3	0
CHOBBr	0	1	1	0
CHOP	0	0	0	50
CHONP	0	0	0	21
CHOSP	0	0	0	1
Total	7768	9039	9143	4862

Table S18. Number and percent of unique formulas for the *Active LL*, *Closed LL*, *Closed-Brine LL*, and *Closed and Closed-Brine LLs* combined.

	Active LL	Closed LL	Closed-Brine LL	Closed and Closed-Brine LLs
Unique	857 (11.0%)	220 (2.4%)	297 (3.2%)	2516 (26.7%)
Total	7768	9039	9143	9427

Other Halogenated Formula Classes

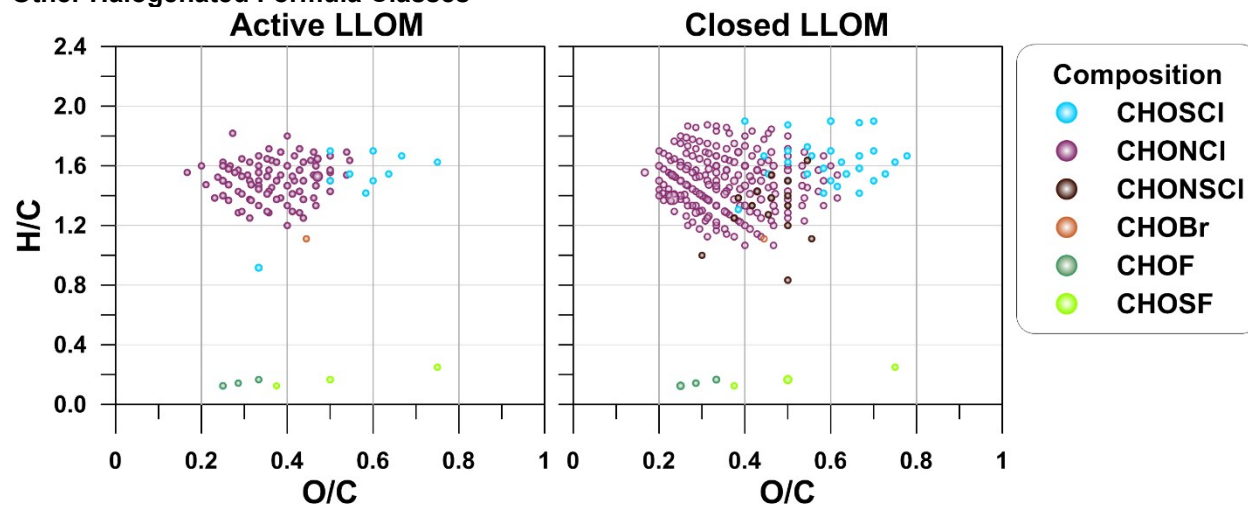


Figure S5. Van Krevelen diagrams of other halogenated formula assignments in the *Active* and *Closed* LL samples. Point size corresponds to signal intensity.

Additional Van Krevelen Diagrams

Van Krevelen plotting in this section was done with the R package ggplot2.⁷

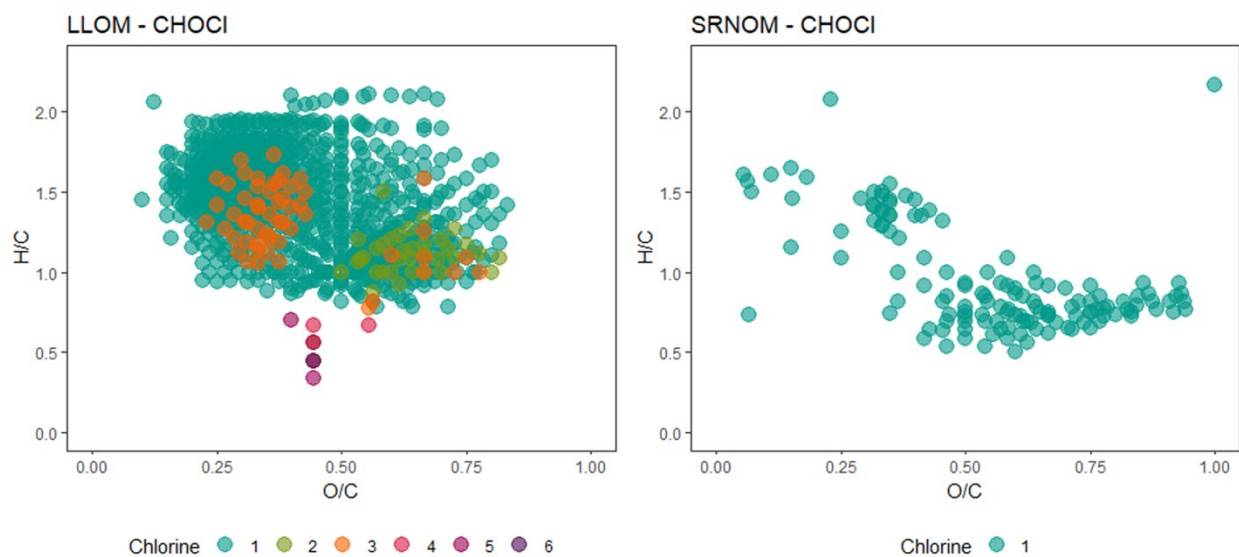


Figure S6. Van Krevelen diagrams of CHOCI formula assignments for LLOM (across all samples) and SRNOM.

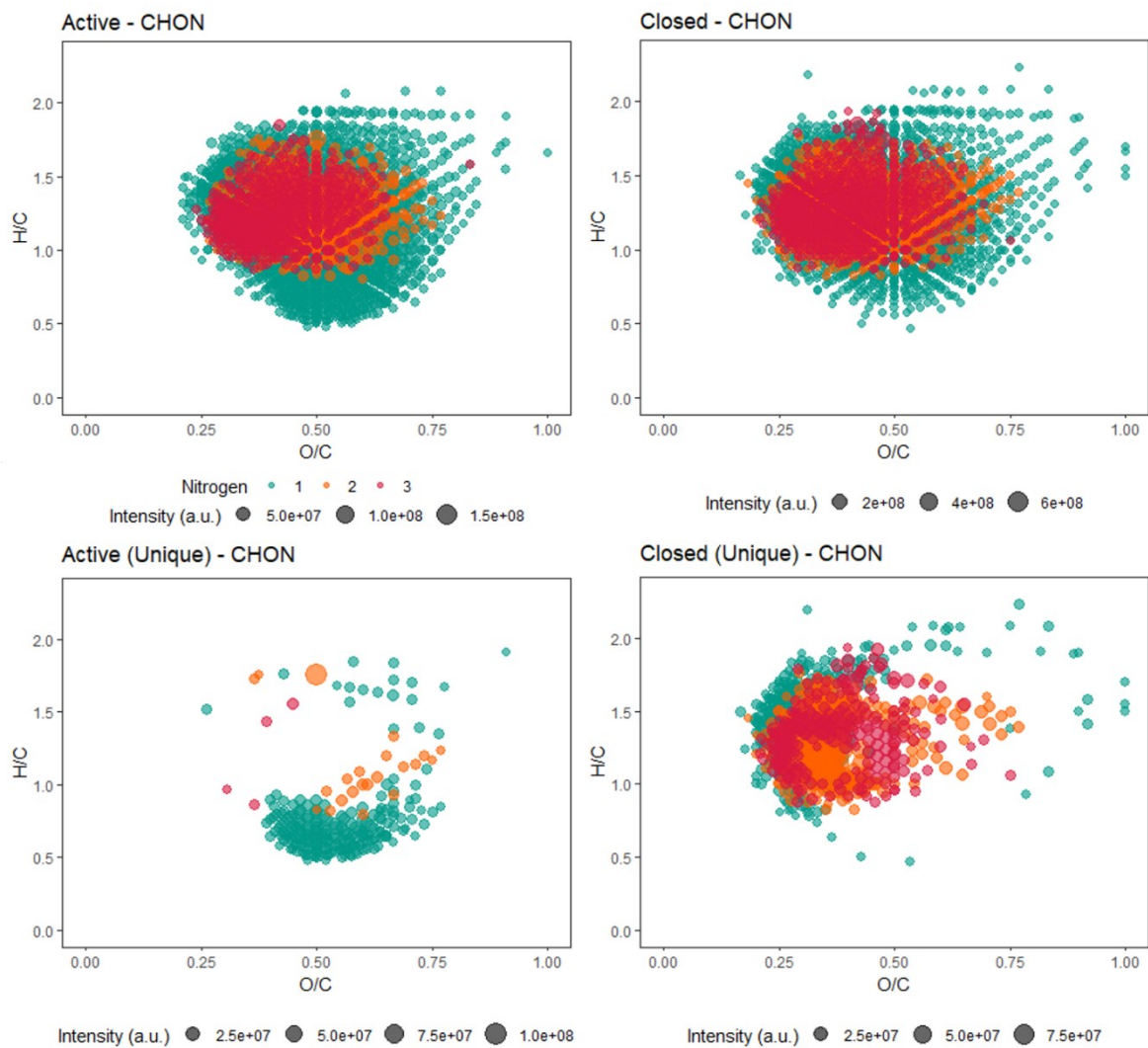


Figure S7. Van Krevelen diagrams of CHON and unique CHON formula assignments for *Active* and *Closed* LL by nitrogen number.

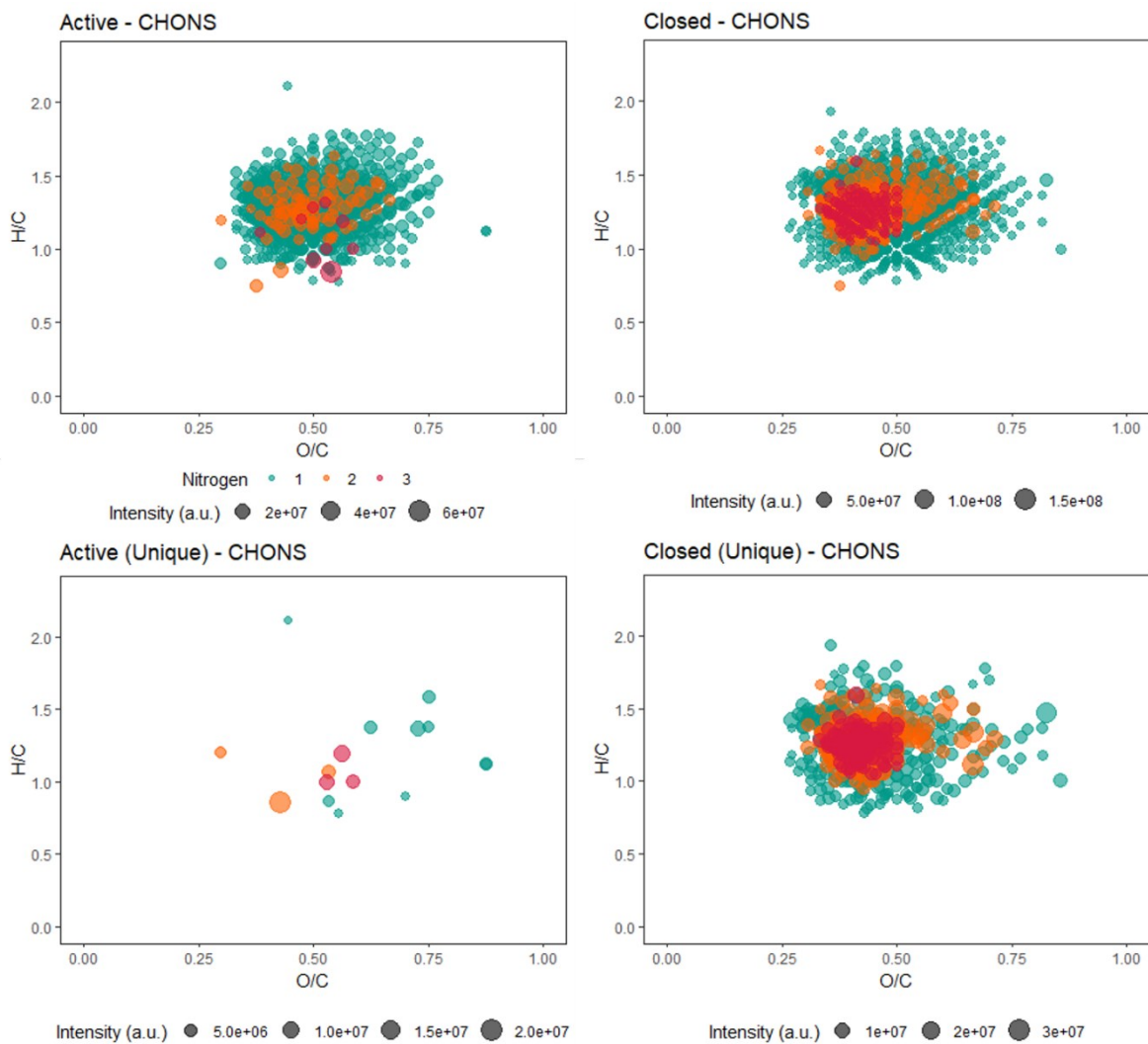


Figure S8. Van Krevelen diagrams of CHONS and unique CHONS formula assignments for *Active* and *Closed* LL by nitrogen number.

C₉H₄Cl₆O₄ and Similar Formula Organohalogenes

Table S19. Signal intensity data in arbitrary units from the unprocessed data matrix to show isotopic patterns which were checked for assignment accuracy with the web interface by Loos et al.⁸ Formulas are protonated, as assigned in the dataset, assuming deprotonated, singly charged, [M-H]⁻ ions. Isotopic composition is as assigned for ions.

Table S20. Averaged signal intensity data in arbitrary units for the most abundant isotopic peak corresponding to the formula. Formulas are ordered from lowest (left) to highest (right) m/z . We believe that $C_9H_5Cl_3O_4$, $C_9H_4Cl_4O_4$, and $C_9H_3Cl_5O_4$ may not be present in the samples and are instead misidentified $[M-HCl-H]^-$ in-source fragmentation products of $C_9H_6Cl_4O_4$, $C_9H_5Cl_5O_4$, and $C_9H_4Cl_6O_4$. These signals theorized to correspond based on signal correlation and in MS behavior are highlighted by color, with the darker shaded title believed to be the false assignment. Removing likely misidentified, in-source fragmentation products, lower m/z formulas within the suite generally had higher signal intensity or were only identified in the *Closed* and *Closed-Brine* LL samples.

Sample	C9H5Cl3O4	C9H7Cl3O5	C9H4Cl4O4	C9H9Cl3O6	C9H6Cl4O4	C9H9Cl3O7	C9H6Cl4O5	C9H10Br2O4	C9H3Cl5O4	C9H5Cl5O4	C10H7Cl5O4	C9H4Cl6O4
Active	0	1594058	19376903	0	4606337	0	9341295	2362062	7874511	397367552	8218451	43443343
Closed	3909314	9613050	9631076	11093412	75523773	4761892	14029617	4709426	0	236772341	6909648	0
Closed-Brine	4112809	9657395	9201891	11429499	77812045	4917851	15553948	3538799	0	257399536	6976435	0

Likely Brominated Ions Not Included in Final Dataset

Table S21. Signal intensity data in arbitrary units from the unprocessed data matrix showing brominated formulas likely present in LLOM that were not included in the final dataset because low signal intensity meant only the higher abundance isotopic peaks, and not the monoisotopic peaks, were visible across triplicates in the data matrix. Signal intensities match expected isotopic patterns.

$C_9H_6Br_2O_2$																				
m/z (avg.)	Closed 3	Closed 2	Closed 1	Closed-Brine 3	Closed-Brine 2	Closed-Brine 1	Active 3	Active 2	Active 1	C12	C13	H	O	Cl35	Cl37	Br79	Br81	Mass Diff (Da)	Error (ppm)	
304.88181	2788389	0	0	0	0	0	0	0	0	0	9	0	7	2	0	0	2	0	-0.00002	0.06
306.87977	4603449	5346732	4501178	3819168	4848689	3748343	0	0	0	0	9	0	7	2	0	0	1	1	-0.00001	0.05
308.87771	2743103	2655747	2825467	0	0	0	0	0	0	0	9	0	7	2	0	0	0	2	-0.00002	0.08
$C_9H_5Br_2O_2$																				
m/z (avg.)	Closed 3	Closed 2	Closed 1	Closed-Brine 3	Closed-Brine 2	Closed-Brine 1	Active 3	Active 2	Active 1	C12	C13	H	O	Cl35	Cl37	Br79	Br81	Mass Diff (Da)	Error (ppm)	
344.75897	3676267	3478216	4453000	3435554	3619724	2738775	2699892	2956657	0	6	0	2	2	0	0	2	1	0	-0.00003	0.07
346.75696	3807650	4761636	3823075	3489118	4171218	3631820	0	0	0	6	0	2	2	0	0	1	2	0	0.00001	0.03

MS settings for QqQ HPLC-MS-MS Experiments

Table S22. MS settings for QqQ HPLC-MS-MS Experiments.

Parameter	Setting
Ion source	ESI
Capillary voltage	-3600 V
Gas temperature	350 °C
Gas flow	8 L/min
Nebulizer gas pressure	25 psi
MS1/MS2 resolution	Unit
Time filtering	peak width = 0.03 min
FV	110 V
CAV	2 V

Targeted QqQ HPLC-MS-MS Experiments

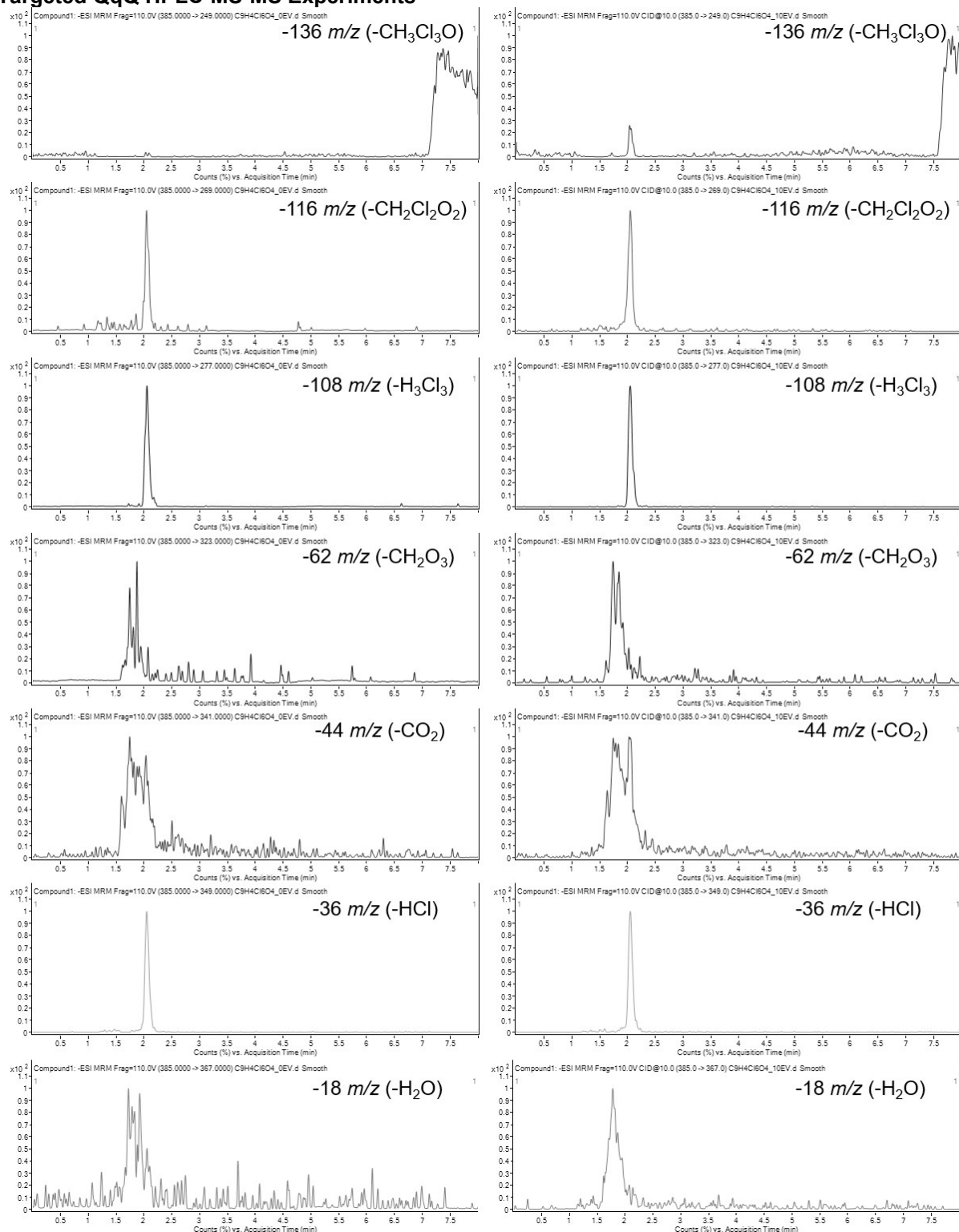


Figure S9. Smoothed chromatograms of QqQ CID HPLC-MS-MS experiments in MRM mode showing monitored transitions at 0 eV (left) and 10 eV (right) CEs for the 384.8 m/z ion, assigned $\text{C}_9\text{H}_4\text{Cl}_6\text{O}_4$, in the Active LL sample. Fragments corresponding to loss of $-\text{CH}_2\text{Cl}_2\text{O}_2$, $-\text{H}_3\text{Cl}_3$, and $-\text{HCl}$ were found at 0 eV at the 2.05 min RT. Fragments corresponding to loss of $-\text{CH}_3\text{Cl}_3\text{O}$, $-\text{CH}_2\text{Cl}_2\text{O}_2$, $-\text{H}_3\text{Cl}_3$, and $-\text{HCl}$ were found at 10 eV at the RT. The loss of $-\text{CO}_2$ may also occur at both 0 and 10 eV, but this could not be fully

resolved from the background. The y-axis represents counts as % base peak, so displayed peak size is not reflective of size as raw counts.

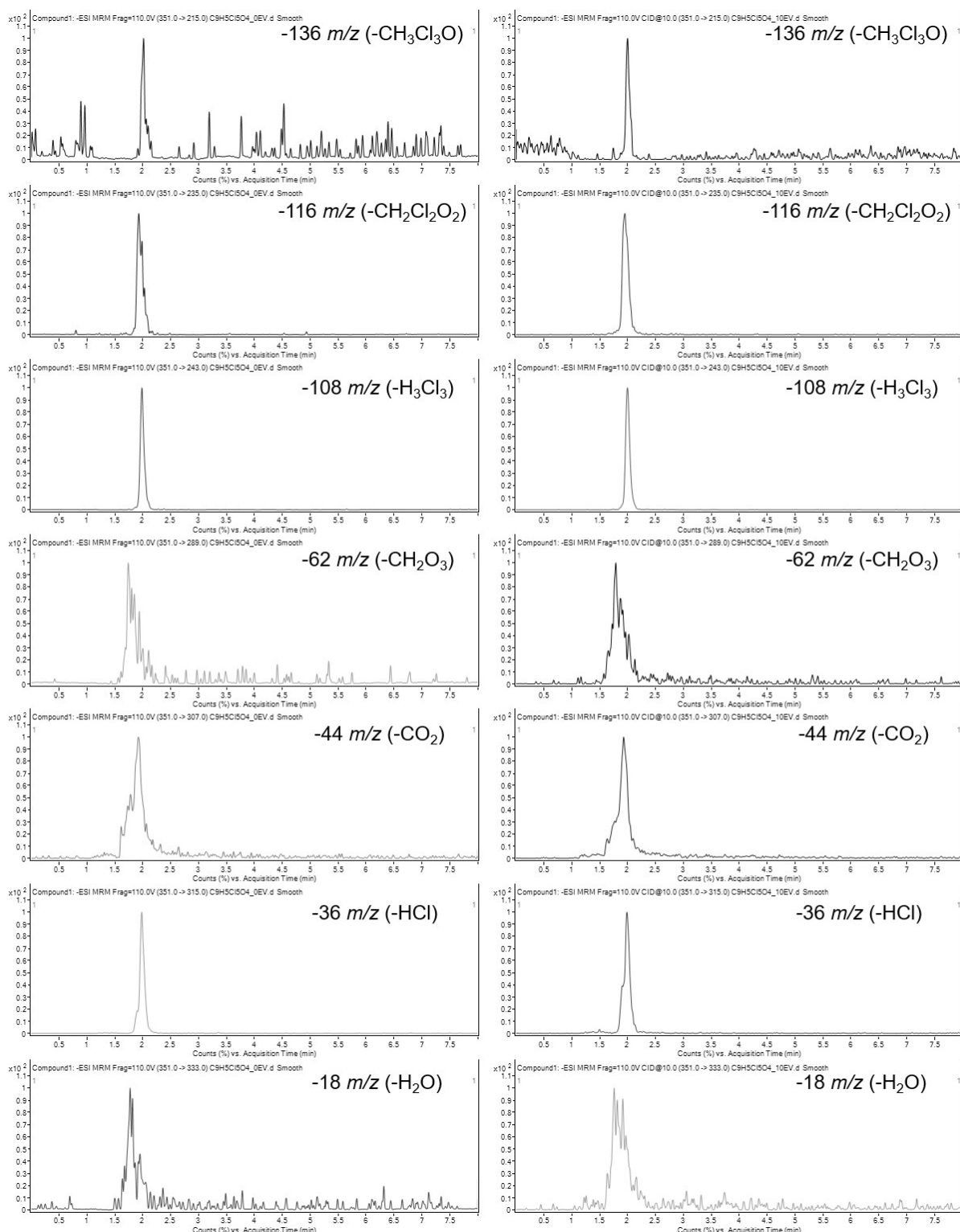


Figure S10. Smoothed chromatograms of QqQ CID HPLC-MS-MS experiments in MRM mode showing monitored transitions at 0 eV (left) and 10 eV (right) CE for the 350.9 m/z ion, assigned $\text{C}_9\text{H}_5\text{Cl}_5\text{O}_4$, in the Active LL sample. Fragments corresponding to loss of $-\text{CH}_3\text{Cl}_3\text{O}$, $-\text{CH}_2\text{Cl}_2\text{O}_2$, $-\text{H}_3\text{Cl}_3$, $-\text{CO}_2$, and $-\text{HCl}$ were

found at 0 and 10 eV at the 1.98 min RT. Analyses of the 350.9 m/z ion in the *Closed LL* sample showed the same results. The y-axis represents counts as % base peak, so displayed peak size is not reflective of size as raw counts.

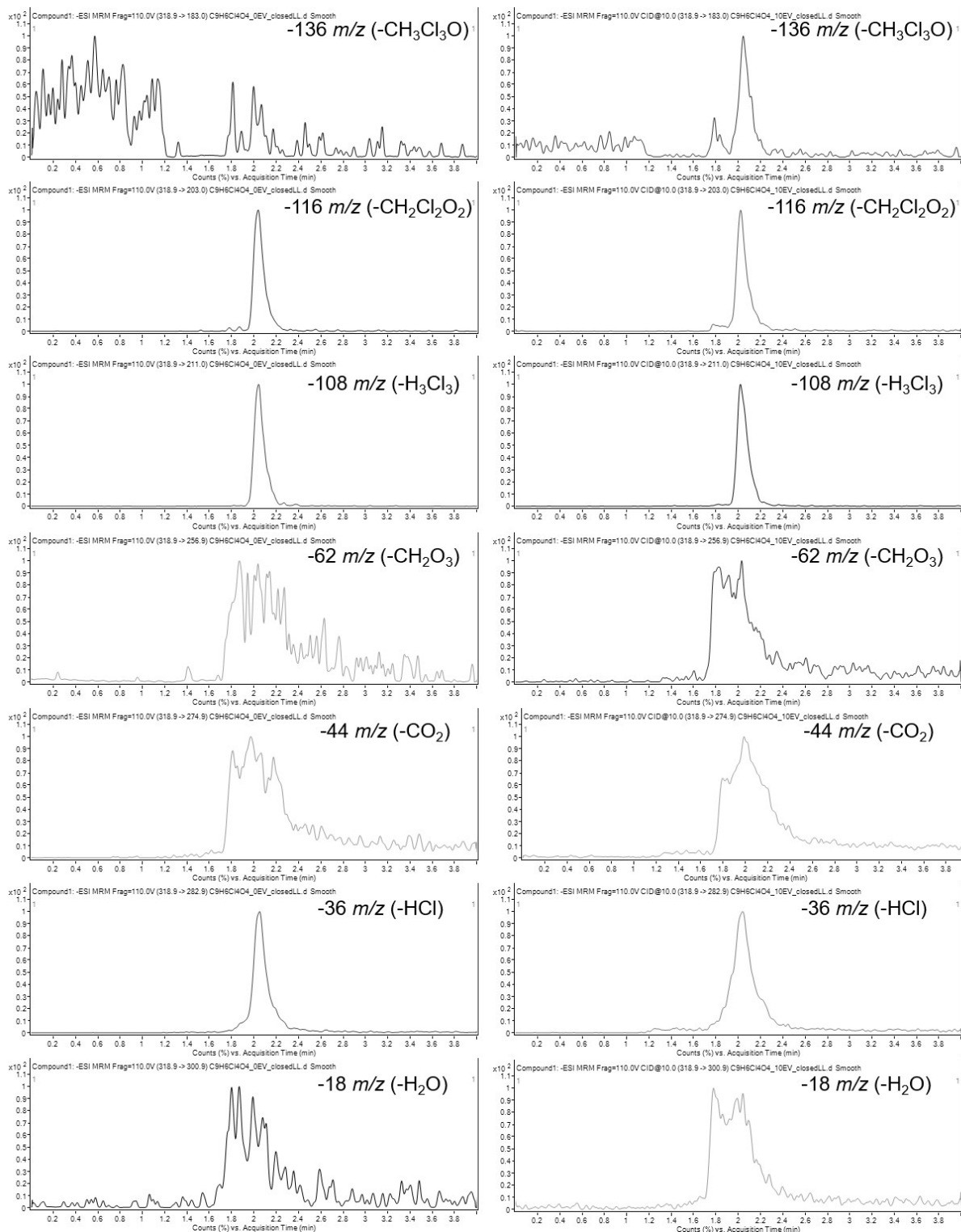


Figure S11. Smoothed chromatograms of QqQ CID HPLC-MS-MS experiments in MRM mode showing monitored transitions at 0 eV (left) and 10 eV (right) CEs for the 318.9 m/z ion, assigned $\text{C}_9\text{H}_6\text{Cl}_4\text{O}_4$, in the

Closed LL sample. Fragments corresponding to loss of $-\text{CH}_2\text{Cl}_2\text{O}_2$, $-\text{H}_3\text{Cl}_3$, and $-\text{HCl}$ were found at 0 eV at the 2.02 min RT. Fragments corresponding to loss of $-\text{CH}_3\text{Cl}_3\text{O}$, $-\text{CH}_2\text{Cl}_2\text{O}_2$, $-\text{H}_3\text{Cl}_3$, and $-\text{HCl}$ were found at 10 eV at the RT. The y-axis represents counts as % base peak, so displayed peak size is not reflective of size as raw counts.

Full Scan Mode QqQ HPLC-MS-MS Experiments

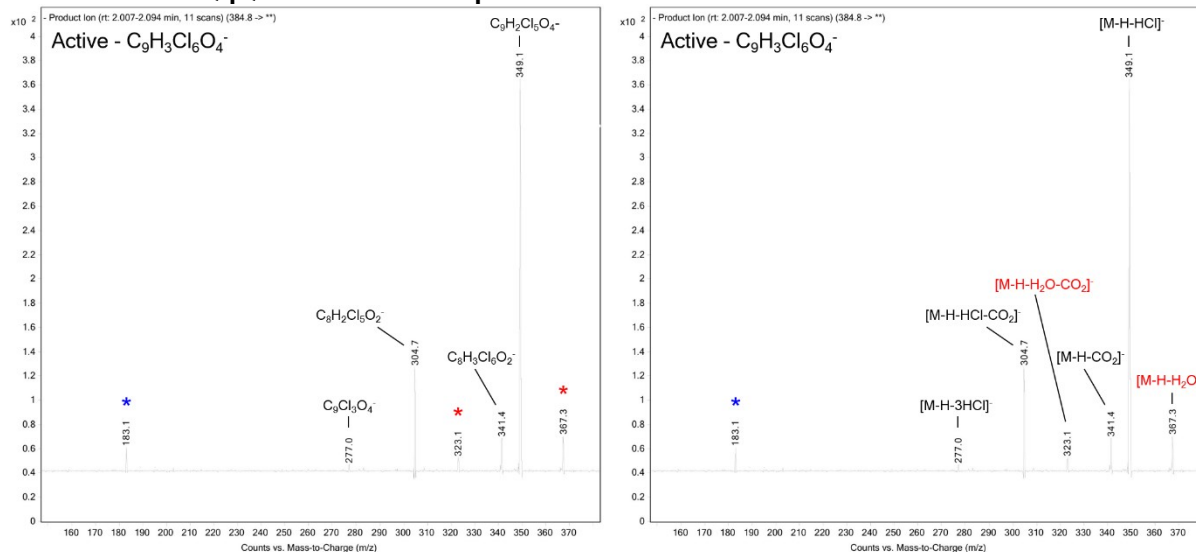


Figure S12. HPLC-MS-MS, full scan mode CID spectrum at 10 eV CE of 384.8 m/z ion, assigned $\text{C}_9\text{H}_4\text{Cl}_6\text{O}_4$, in the Active LL sample by QqQ MS. Spectrum is average of 11 scans at approximate 2.05 min RT. Fragment identification (left) and possible corresponding neutral losses (right) are shown. Red asterisks and text mark common background fragments that were present throughout the run. The blue asterisk marks an unidentified fragment at the RT that may be unrelated. Low mass resolution and error is typical of a QqQ MS operating in full scan mode.

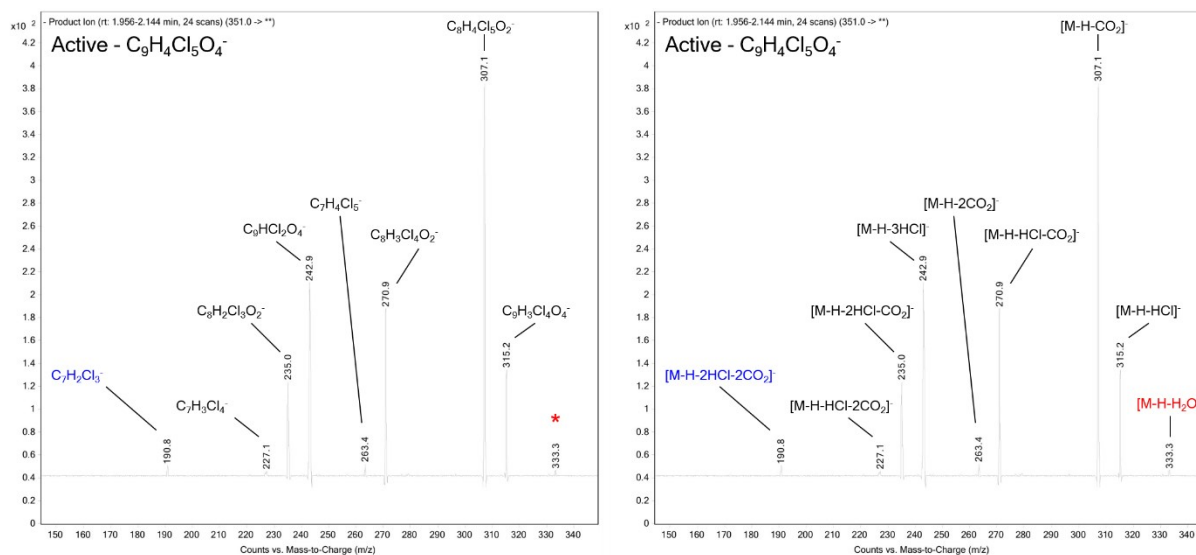


Figure S13. HPLC-MS-MS, full scan mode CID spectrum at 10 eV CE of 350.9 m/z ion, assigned $\text{C}_9\text{H}_5\text{Cl}_5\text{O}_4$, in the Active LL sample by QqQ MS. Spectrum is average of 24 scans at approximate 1.98 min RT. Fragment identification (left) and possible corresponding neutral losses (right) are shown. The red asterisk and text marks a common background fragment that was present throughout the run. The blue text marks a fragment at the RT that may be unrelated.

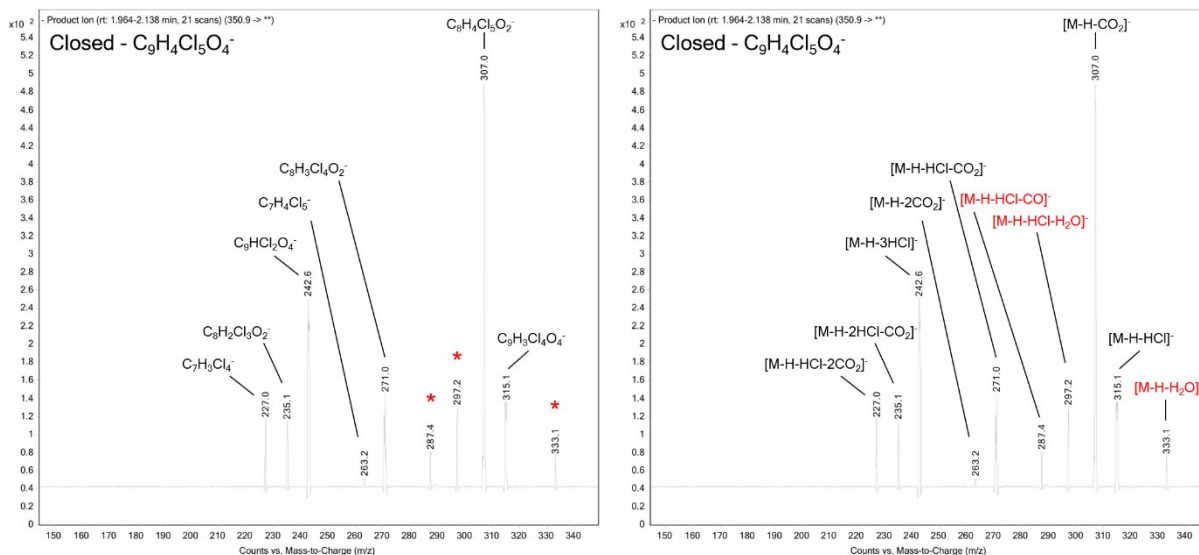


Figure S14. HPLC-MS-MS, full scan mode CID spectrum at 10 eV CE of 350.9 m/z ion, assigned $C_9H_5Cl_5O_4$, in the *Closed* LL sample by QqQ MS. Spectrum is average of 21 scans at approximate 1.98 min RT. Fragment identification (left) and possible corresponding neutral losses (right) are shown. The red asterisks and text mark background fragments that were present throughout the run.

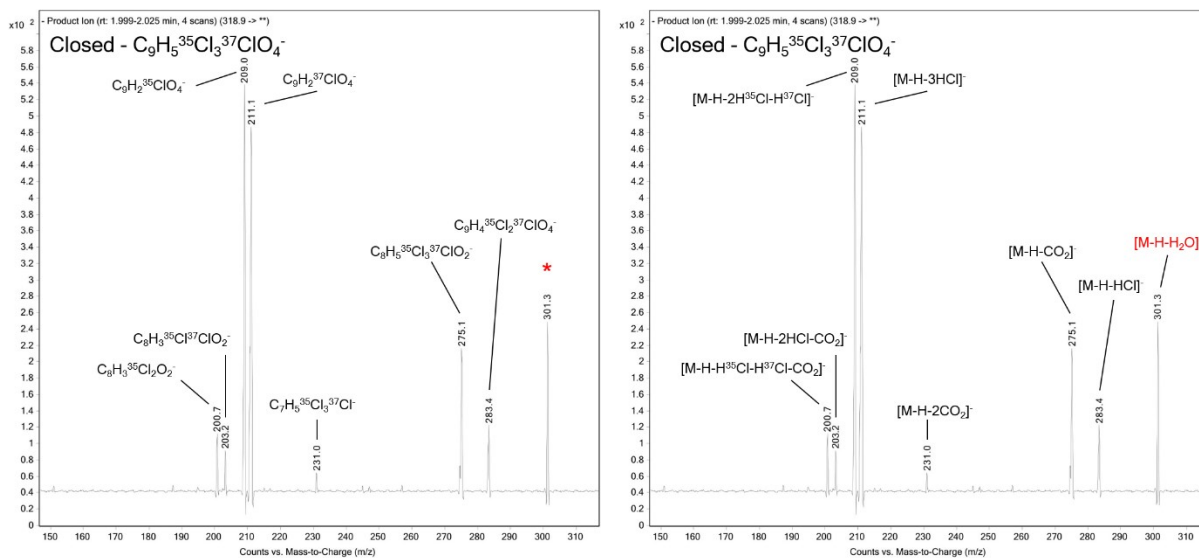


Figure S15. HPLC-MS-MS, full scan mode CID spectrum at 10 eV CE of 318.9 m/z ion in the *Closed* LL sample by QqQ MS. The corresponding monoisotopic ion (316.9 m/z) was assigned $C_9H_6Cl_4O_4$. Spectrum is average of 4 scans at approximate 2.02 min RT. Fragment identification (left) and possible corresponding neutral losses (right) are shown. The red asterisk and text marks a common background fragment that was present throughout the run.

Orbitrap MS-MS Experiments

Table S23. Ion lists of 20 highest intensity peaks from direct injection Orbitrap MS-MS on the highest abundance chlorine isotopic peak of $C_9H_5Cl_5O_4$ (352.85 m/z) in the *Active* sample. Mass resolution was 15,000, fragmentation was by CID at CE of 0 (left) and 10 eV (right) in full scan mode using the FTMS (Orbitrap) detector, recording 0.4 min long scan averages. Fragments identified as related to the parent compound are highlighted. Fragmentation of other isotopic peaks (350.86 and 354.85 m/z) showed the same fragment formation following expected isotopic patterns.

FTMS - p ESI Full ms2 352.85@cid0.00 [95.00-353.00]					FTMS - p ESI Full ms2 352.85@cid10.00 [95.00-353.00]					
Scan #: 1-37					Scan #: 1-36					
RT: 0.01-0.41					RT: 0.01-0.40					
AV: 37					AV: 36					
m/z	Intensity	Relative	Formula	Loss	m/z	Intensity	Relative	Formula	Loss	Possible Neutral Loss
108.5925	223.1	0.22			101.6826	201.6	0.77			
173.91633	204.4	0.2			103.52215	199.8	0.76			
175.83216	229.1	0.22			109.22732	189.7	0.72			
185.81465	196.8	0.19			124.21209	191.7	0.73			
197.2459	544.4	0.53			168.59209	289.1	1.1			
203.70446	724.4	0.7			186.02932	196.1	0.75			
254.26967	2268.9	2.19			203.7062	562.7	2.15			
273.65148	2723	2.63			215.3538	188.4	0.72			
277.43503	196.3	0.19			228.48514	203.5	0.78			
283.90569	324.2	0.31			234.91095	1008.1	3.84	$C_8H_2^{35}Cl_3O_2^-$	$CH_3^{35}Cl^{37}ClO_2$	$H + H^{35}Cl + H^{37}Cl + CO_2$
340.56887	209.5	0.2			236.90795	1511	5.76	$C_8H_2^{35}Cl_2^{37}ClO_2^-$	$CH_3^{35}Cl_2O_2$	$H + 2H^{35}Cl + CO_2$
352.51528	278.6	0.27			254.26993	1796.3	6.85			
352.53105	1292.7	1.25			272.88436	587.8	2.24			
352.53751	1388.9	1.34			273.65167	2672.8	10.19			
352.55891	694.3	0.67			274.32805	200.5	0.76			
352.57894	631	0.61			308.86059	4263	16.26	$C_8H_4^{35}Cl_4^{37}ClO_2^-$	CHO_2	$H + CO_2$
352.61113	3170.1	3.06			309.03692	240.5	0.92			
352.68417	248.9	0.24			316.87382	3869.9	14.76	$C_9H_3^{35}Cl_3^{37}ClO_4^-$	$H_2^{35}Cl$	$H + H^{35}Cl$
352.85068	103591	100	$C_9H_4^{35}Cl_4^{37}ClO_4^-$	H	352.61152	3912.6	14.92			
352.993	315.5	0.3			352.85062	26220.5	100	$C_9H_4^{35}Cl_4^{37}ClO_4^-$	H	H

Table S24. Ion lists of 20 highest intensity peaks from direct injection Orbitrap MS-MS on the highest abundance chlorine isotopic peak ($C_9H_4Cl_6O_4$, 386.81 m/z) of the 100 $\mu g/L$ chlorendic acid standard solution, made with a chlorendic acid standard (Sigma-Aldrich, 99%) and ultrapure water. Mass resolution was 15,000, fragmentation was by CID at CEs of 0 eV (top left), 10 eV (top right), 20 eV (bottom left), and 60 eV (bottom right) in full scan mode using the FTMS (Orbitrap) detector, recording 0.4 min long scan averages. Fragmentation of other isotopic peaks (384.82, 388.81, and 390.81 m/z) showed the same fragment formation following expected isotopic patterns.

FTMS - p ESI Full ms2 386.81@cid0.00 [105.00-387.00]					FTMS - p ESI Full ms2 386.81@cid10.00 [105.00-387.00]					Possible Neutral Loss	
m/z	Intensity	Relative	Formula	Loss	m/z	Intensity	Relative	Formula	Loss		
109.9198	188.4	1.65			119.556	224.5	2.88				
120.4691	247.2	2.16			119.7411	233.1	2.98				
129.7376	207.2	1.81			128.048	244	3.12				
134.1164	190.3	1.66			173.9636	280.9	3.6				
156.2447	198.8	1.74			190.8639	237.5	3.04				
163.0515	221	1.93			195.8224	246.3	3.15				
184.6679	177.4	1.55			198.3531	247.6	3.17				
188.6685	237.6	2.08			207.5571	244.2	3.13				
200.3261	197.2	1.72			253.4998	299.6	3.84				
228.8981	221.5	1.94			273.665	4442.1	56.89				
273.665	4325.8	37.84			278.8823	421.3	5.4	$C_9^{35}Cl_2^{37}ClO_4^-$	$H_4^{35}Cl_3$	$H+3H^{35}Cl$	
313.8162	250	2.19			317.2019	228.6	2.93				
379.6384	283.6	2.48			348.8389	750.2	9.61	$C_9H_2^{35}Cl_5O_4^-$	$H_2^{37}Cl$	$H+H^{37}Cl$	
379.6678	1727.5	15.11			350.8356	7808.2	100	$C_9H_2^{35}Cl_4^{37}ClO_4^-$	$H_2^{35}Cl$	$H+H^{35}Cl$	
379.6825	2439.6	21.34			379.6528	367.2	4.7				
379.6928	2734.4	23.92			379.6815	2863.6	36.68				
379.7012	2579.1	22.56			379.6928	3312.3	42.42				
379.7179	1464.5	12.81			379.703	2467.6	31.6				
386.7147	508.5	4.45			379.7114	2250.6	28.82				
386.8127	11431.4	100	$C_9H_3^{35}Cl_5^{37}ClO_4^-$	H	386.8127	2160.8	27.67	$C_9H_3^{35}Cl_5^{37}ClO_4^-$	H	H	
FTMS - p ESI Full ms2 386.81@cid20.00 [105.00-387.00]					FTMS - p ESI Full ms2 386.81@cid60.00 [105.00-387.00]						
Scan #: 1-19					Scan #: 1-19						
RT: 0.01-0.39					RT: 0.01-0.39						
AV: 19					AV: 19						
m/z	Intensity	Relative	Formula	Loss	Possible Neutral Loss	m/z	Intensity	Relative	Formula	Loss	Possible Neutral Loss
119.5662	245.5	1.85				111.838	177.1	3.24			
167.9652	180.8	1.36				117.6897	187.9	3.44			
204.4308	175.7	1.33				119.9337	175.4	3.21			
214.0743	259.6	1.96				126.1023	226	4.13			
253.5	1079.3	8.14				136.6582	233.2	4.26			
270.8693	226.4	1.71	$C_8H^{35}Cl_3^{37}ClO_2^-$	$CH_3^{35}Cl_2O_2$	$H+2H^{35}Cl+CO_2$	253.4995	349.2	6.39			
273.6649	3646.1	27.51				266.25	260.2	4.76			
276.0752	178	1.34				273.665	3528.3	64.53			
278.8817	297.1	2.24	$C_9^{35}Cl_2^{37}ClO_4^-$	$H_4^{35}Cl_3$	$H+3H^{35}Cl$	276.8848	538.3	9.84	$C_9^{35}Cl_3O_4^-$	$H_4^{35}Cl_2^{37}Cl$	$H+2H^{35}Cl+H^{37}Cl$
282.3669	244.5	1.84				277.427	177.9	3.25			
283.9194	339	2.56				278.8826	301.3	5.51	$C_9^{35}Cl_2^{37}ClO_4^-$	$H_4^{35}Cl_3$	$H+3H^{35}Cl$
306.7672	178.1	1.34				305.127	176.6	3.23			
348.8385	1339.1	10.1	$C_9H_2^{35}Cl_5O_4^-$	$H_2^{37}Cl$	$H+H^{37}Cl$	348.8383	846.5	15.48	$C_9H_2^{35}Cl_5O_4^-$	$H_2^{37}Cl$	$H+H^{37}Cl$
350.8359	13252.3	100	$C_9H_2^{35}Cl_4^{37}ClO_4^-$	$H_2^{35}Cl$	$H+H^{35}Cl$	350.8357	5468	100	$C_9H_2^{35}Cl_4^{37}ClO_4^-$	$H_2^{35}Cl$	$H+H^{35}Cl$
351.2254	176.2	1.33				351.4641	235.7	4.31			
379.622	181.8	1.37				357.4682	257.2	4.7			
379.6432	329.5	2.49				379.6369	267.4	4.89			
379.6698	1895.2	14.3				379.6422	296.7	5.43			
379.6899	4483.2	33.83				379.6856	5204.8	95.18			
379.7202	974.6	7.35				379.7313	281.7	5.15			

References

1. M. S. Twardowski, E. Boss, J. M. Sullivan and P. L. Donaghay, Modeling the spectral shape of absorption by chromophoric dissolved organic matter, *Mar. Chem.*, 2004, **89**, 69-88.
2. J. L. Weishaar, G. R. Aiken, B. A. Bergamaschi, M. S. Fram, R. Fujii and K. Mopper, Evaluation of specific ultraviolet absorbance as an indicator of the chemical composition and reactivity of dissolved organic carbon, *Environ. Sci. Technol.*, 2003, **37**, 4702-4708.
3. B. P. Koch, T. Dittmar, M. Witt and G. Kattner, Fundamentals of molecular formula assignment to ultrahigh resolution mass data of natural organic matter, *Anal. Chem.*, 2007, **79**, 1758-1763.
4. P. Herzprung, N. Hertkorn, W. von Tümpling, M. Harir, K. Friese and P. Schmitt-Kopplin, Understanding molecular formula assignment of Fourier transform ion cyclotron resonance mass spectrometry data of natural organic matter from a chemical point of view, *Anal. Bioanal. Chem.*, 2014, **406**, 7977-7987.
5. A. McMillan, J. B. Renaud, G. B. Gloor, G. Reid and M. W. Sumarah, Post-acquisition filtering of salt cluster artefacts for LC-MS based human metabolomic studies, *J. Cheminformatics*, 2016, **8**, 1-5.
6. J. D. Rogers, E. M. Thurman, I. Ferrer, J. S. Rosenblum, M. V. Evans, P. J. Mouser and J. N. Ryan, Degradation of polyethylene glycols and polypropylene glycols in microcosms simulating a spill of produced water in shallow groundwater, *Environ. Sci. Process. Impacts*, 2019, **21**, 256-268.
7. H. Wickham, *ggplot2: elegant graphics for data analysis*, Springer-Verlag, New York, 2016.
8. M. Loos, C. Gerber, F. Corona, J. Hollender and H. Singer, Accelerated isotope fine structure calculation using pruned transition trees, *Anal. Chem.*, 2015, **87**, 5738-5744.